

## Enhanced Performance in Inductive Wireless Energy Transfer Systems: A Study of Helical and Tubular Coils Configurations

Mohammed Wadi<sup>1\*</sup>, Mohammed Salemdceb<sup>2</sup>, Mohammed Jouda<sup>3</sup> and Riad Bendib<sup>4</sup>

<sup>1</sup>Electrical Electronics Dept., Istanbul Zaim Sabahattin Uni, Türkiye  
(ORCID: <https://orcid.org/0000-0001-8928-3729>)

<sup>2</sup>Electrical Electronics Dept., Istanbul Zaim Sabahattin Uni, Türkiye  
(ORCID: <https://orcid.org/0000-0002-2913-7671>)

<sup>3</sup>Electrical Electronics Dept., Istanbul Zaim Sabahattin Uni, Türkiye  
(ORCID: <https://orcid.org/0000-0002-7364-5059>)

<sup>4</sup>Laboratory of Automatic, Skikda University, Algeria  
(ORCID: <https://orcid.org/0000-0003-4677-1639>)

\*([mohammed.wadi@izu.edu.tr](mailto:mohammed.wadi@izu.edu.tr))

(Received: 02 June 2025, Accepted: 04 June 2025)

(5th International Conference on Contemporary Academic Research ICCAR 2025, May 30-31, 2025)

**ATIF/REFERENCE:** Wadi, M., Salemdceb, M., Joudaa, M. & Bendib, R. (2025). Enhanced Performance in Inductive Wireless Energy Transfer Systems: A Study of Helical and Tubular Coils Configurations. *International Journal of Advanced Natural Sciences and Engineering Researches*, 9(6), 100-108.

**Abstract** – This paper presents the simulation and comparative analysis of different coil geometries used in wireless power transfer systems, focusing on square and spiral coil configurations. Using the Ansys Maxwell 3D simulation environment, key electromagnetic parameters such as self-inductance, mutual inductance, and coupling coefficients were calculated to evaluate the performance of each design. This study examines two coil geometries' inductive and magnetic coupling characteristics—helical and tubular—across different separation lengths. Inductance and coupling coefficient values were derived via simulations using self- and mutual-inductance matrices. The helical coil demonstrated a coupling coefficient of around 0.086 and an inductance of 83.4  $\mu\text{H}$  at a spacing of 135 mm. The self-inductance values of the tubular coil exhibited slight fluctuation with distance, affirming that self-inductance is primarily independent of coil separation. Conversely, mutual inductance and coupling coefficients markedly decreased as the inter-coil distance rose, with the tubular coil's coupling coefficient declining from 0.276 at 50 mm to 0.038 at 200 mm. These findings validate the susceptibility of magnetic coupling to coil configuration and separation, offering valuable insights for wireless power transmission and magnetic sensing applications.

**Keywords** – Wireless Energy Transfer, Inductive Coupling, Wireless Power Transfer, Ansys Maxwell 3D Simulation, Helical Coil, Tubular Coil.

### I. INTRODUCTION

Wireless energy transfer is the transfer of electrical energy without any physical conductor [1]. This method of energy transfer has been an area of study for many years, with research focusing on ensuring the

efficient transmission of energy through wireless means. Inductive coupling, first developed by Tesla, has been instrumental in applying wireless energy in various fields, including electronics, healthcare, and industry. This technology has dramatically enhanced convenience in our daily lives through high-frequency and semiconductor technology. The use of wireless energy transfer has reduced the complexities associated with physical connections, providing various advantages to the end user. The charging of modern technological devices, such as phones [2], electric toothbrushes, and electric vehicles [3], [4], is now possible through wireless energy transfer.

Inductive coupling is a short-distance wireless energy transmission method more cost-effective and efficient than long-distance wireless energy transmission systems. As a result, it has a wide range of applications. It is commonly used in wet environments, such as electric toothbrushes and shavers, due to its reduced risk of shock and improved ease of use. It is also utilized in medical implants, including pacemakers and insulin pumps, and in charging pads for mobile devices and electric vehicles. This method typically involves the transfer of power between two non-contacting inductor coils, with designs focusing on the electromagnetic field between the coils [5-12].

Efficiency in the power transmission method using inductive coupling can be improved by increasing the operating bandwidth of the inductive coil. This is achieved by adding resonance capacitors to the driver coil, with the resonant frequencies adjusted to the most appropriate frequency range by modifying the capacitor values. Optimum values are set to ensure a constant output signal at the peak reached, with the resonant capacitor essential in obtaining a stable power transfer coefficient and eliminating frequency division [13-20].

Wireless power transfer (WPT) using inductive coupling can pose challenges in meeting output power and efficiency requirements for some applications due to the small coupling coefficient between the transmit and receiver coils. Additionally, the transmission efficiency based on inductive coupling decreases as the coupling factor decreases. In WPT using inductive coupling, four different topologies exist based on the state of the coils in the circuit: series-series, series-parallel, parallel-series, and parallel-parallel. Each has advantages and disadvantages, with the efficiency of parallel-parallel and series-parallel topologies higher at low frequencies and the serial-to-serial topology more efficient than others at high frequencies. The serial-to-serial topology is the most widely used method, both theoretically and practically, especially at low powers [21-31].

This paper aims to investigate various WPT methods, followed by the design and analysis of the system using Maxwell 3D Design simulation program. Based on the analysis results, the circuit will be constructed, and data will be collected and recorded for further evaluation.

## II. MATERIALS AND METHOD

Wireless power transmission with the inductive coupling technique encompasses four distinct topologies determined by the coil arrangement inside the circuit: series-series, series-parallel, parallel-series, and parallel-parallel. Every topology has distinct benefits and drawbacks. The parallel-parallel and series-parallel configurations exhibit greater efficiency at low frequencies, whereas at high frequencies, the series-series configuration demonstrates much superior efficiency compared to the alternatives. The series-series topology is the most prevalent approach conceptually and practically in low-power applications [3].

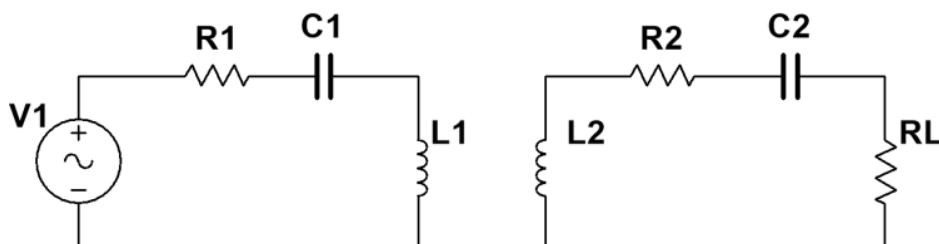


Fig 1. Series-series inductive coupling circuit diagram

Research was done to analyze inductively coupled wireless power transfer systems, focusing on the computation of self-inductance, mutual inductance, and the coupling coefficient. The self-inductance may be determined via Wheeler's formula [32-37]:

$$L = 31.33 \mu_o \left( \frac{N^2 r^2}{8r + 11w} \right) \quad (1)$$

Where,  $N$  signifies the number of turns,  $r$  indicates the average radius, and  $w$  represents the width of the coil.  $\mu_o$  The Biot–Savart Law and Stokes' Theorem may determine the mutual inductance and coupling coefficient. The coupling coefficient ( $k$ ) is determined as follows:

$$k = \frac{M}{\sqrt{L_1 L_2}} \quad (2)$$

where,  $M$  denotes the mutual inductance. The coupling coefficient is inversely related to axial misalignment and the distance separating the coils. As axial misalignment escalates, the coupling coefficient diminishes swiftly, decreasing efficiency [38-47].

#### A. Coil Simulations

The present research involved simulating various coil shapes using the Ansys Electronics simulation program, specifically Maxwell 3D, and comparing the results to determine the optimal coil shape. In particular, the study examined the inductance values ( $L$ ), mutual inductance between two coils ( $M$ ), coupling coefficient ( $k$ ), magnetic fields ( $B$ ), and their respective changes as a function of distance for two different coil types: helical and tubular coils.

#### B. Helical Coil

The parameters chosen for the helical coil developed in Ansys Electronics are shown in Figure 2. Each selected value influences the strength of the magnetic field produced around the wire and the current's efficacy. The design parameters have been selected to align with those of other coils. Figure 3 explains the design of receiver and transmitter helical coils and their view from the -Y axis.

Properties: HelixCoil - Maxwell3DDesign1 - Modeler

Command

Name	Value	Unit	Evaluated Value	Description
Command	CreateUserDefinedPart			
Coordinate System	Global			
Name	SegmentedHelix/PolygonHelix.dll			
Location	syslib			
Version	1.0			
PolygonSegments	0		0	Number of cross-section polygon segments, 0 for circle
PolygonRadius	0.5	mm	0.5mm	Outer radius of cross-section polygon
StartHelixRadius	150	mm	150mm	Start radius from polygon center to helix center
RadiusChange	0	mm	0mm	Radius change per turn
Pitch	1.01	mm	1.01mm	Helix pitch
Turns	44		44	Number of turns
SegmentsPerTurn	36		36	Number of segments per turn, 0 for true surface
RightHanded	1		1	Helix direction, non-zero for right handed

☐ Show Hidden

Tamam İptal Uygula

Fig 2. Parameters used for helical coil design

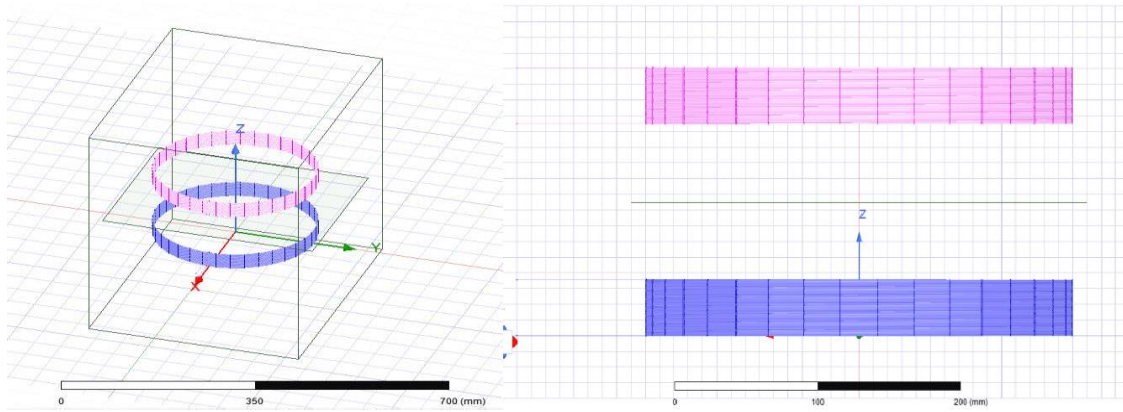


Fig 3. Design of receiver and transmitter helical coils and their view from the -Y axis

### C. Tubular Coil

The specifications for the tubular coil developed in Ansys Electronics are outlined in Figure 4. Each selected value affects the strength of the magnetic field produced around the tube and the current flowing through it in the coil configuration.

Properties: copper pipe - Maxwell3DDesign1 - Modeler

Name	Value	Unit	Evaluated Value	Description
Command	CreateUserDefinedPart			
Coordinate Sys...	Global			
Name	SegmentedHelix/PolygonHelix.dll			
Location	syslib			
Version	1.0			
PolygonSegme...	0		0	Number of cross-section polygon segments, 0 for circle
PolygonRadius	5	mm	5mm	Outer radius of cross-section polygon
StartHelixRadius	180	mm	180mm	Start radius from polygon center to helix center
RadiusChange	0	mm	0mm	Radius change per turn
Pitch	25	mm	25mm	Helix pitch
Turns	1		1	Number of turns
SegmentsPerT...	36		36	Number of segments per turn, 0 for true surface
RightHanded	1		1	Helix direction, non-zero for right handed

☐ Show Hidden

Tamam İptal Uygula

Fig 4. Parameters used for tubular coil design

Figure 5 shows the of receiver and transmitter tubular coils and their view from the -Z axis.

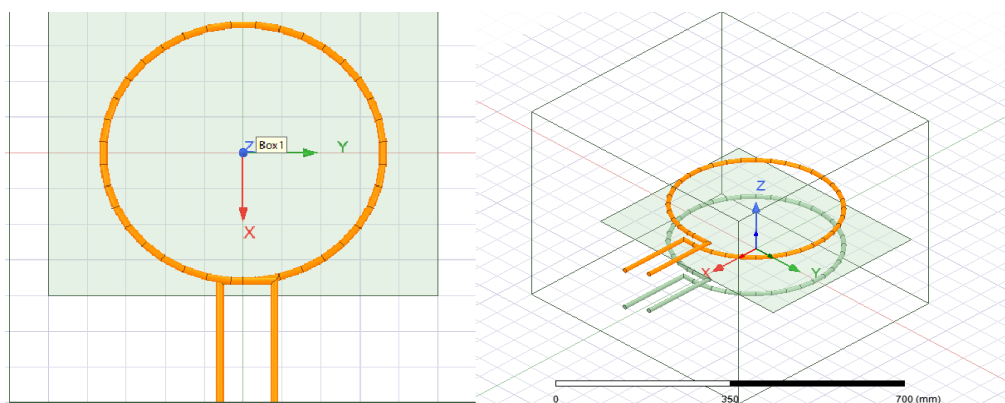


Fig 5. Design of receiver and transmitter tubular coils and their view from the -Z axis

### III. RESULTS & DISCUSSION

Figure 6 shows the operation of the receiver and transmitter circuits together in the wireless power transfer simulation. Since the Multisim simulation software does not offer a feature for coil design, the coils were analyzed using the Ansys program. The inductance values of the tubular coil at 100 millimeters were obtained, and to carry out this wireless power transfer simulation in Multisim, the "inductor coupling" component was used. This allowed for creating a magnetic field simulation that closely resembles real-life conditions. A Zero Voltage Switching (ZVS) driver circuit was used to ensure that the wireless power transfer circuit operates at optimal values and meets system requirements. Due to its ability to handle high currents and frequencies, this circuit can drive many transformers. In the ZVS driver circuit, the ferrite core of the coil repels and attracts the current around the coil. As a result, the ferrite generates an alternating magnetic field, enhancing the receiver coil's inductive performance.

When examining the schematic of the operational circuit, it is observed that the average AC voltage at the terminals of the transmitter circuit is 18.4 volts, and the circuit's operating frequency is measured to be approximately 91.3 kHz. However, it is observed that the average voltage transmitted from the transmitter circuit to the receiver circuit drops to around 2.48 volts. Additionally, the power received at the LED placed at the output of the receiver circuit is measured to be approximately 8.99 watts.

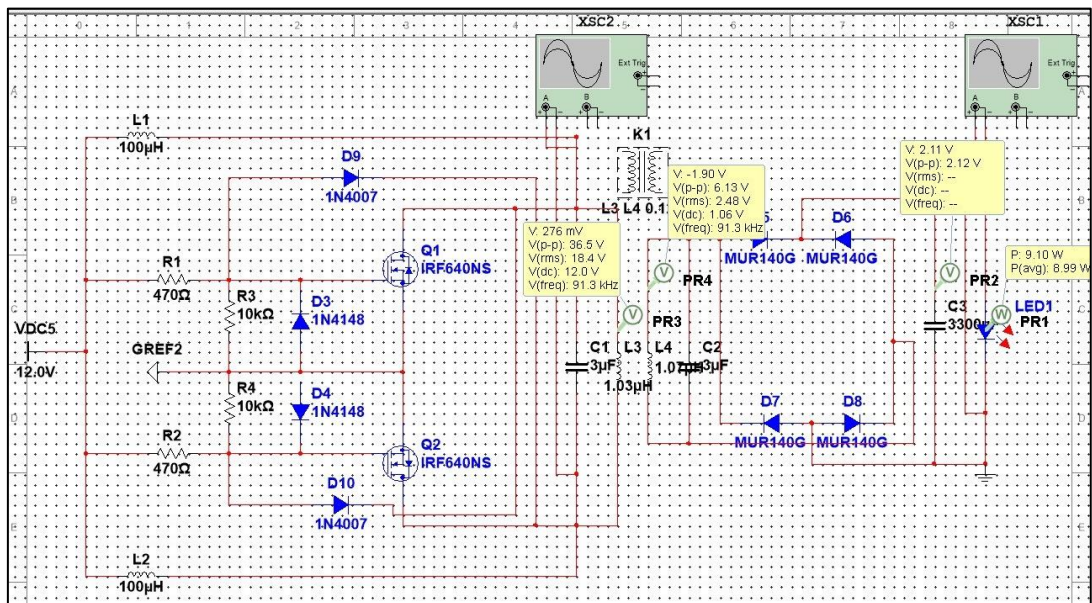


Fig 6. WPT circuit diagram

### A. Helical Coil

Table 1 shows that the coupling coefficient resulting from the magnetic field interaction between two helical coils at 135 millimeters is 0.086, and the inductance value is approximately 83.4 microhenries.

Table1. Inductance values of the helical coil with respect to distance

Dist [mm]	Matrix1.L(Rx_in,Rx_in) [uH]	Matrix1.L(Tx_in,Rx_in) [nH]	Matrix1.L(Rx_in,Tx_in) [nH]	Matrix1.L(Tx_in,Tx_in) [uH]
135	968,335,586	83,408,384	83,408,384	960,922,890

Table 2. Coupling coefficient values of the helical coil

Dist [mm]	Matrix1.CplCoef (Rx_i,Rx_in)	Matrix1.CplCoef (Tx_in,Rx_in)	Matrix1.CplCoef (Rx_in,Tx_in)	Matrix1.CplCoef (Tx_in,Tx_in)
135	1	0.086467	0.086467	1



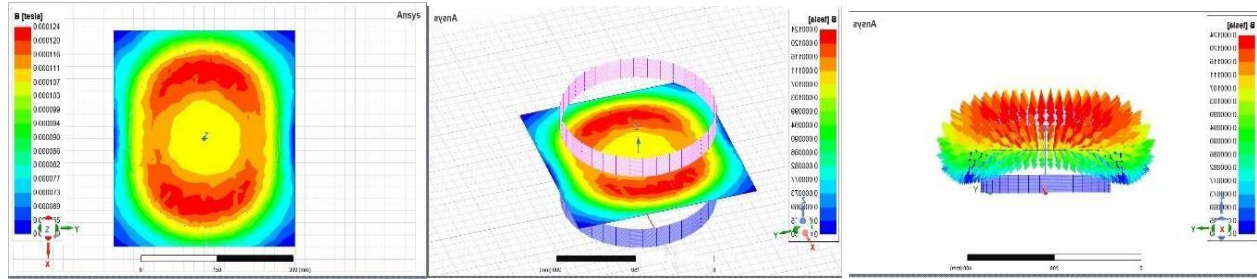


Fig 7. Simulation of magnetic field densities of the helical coil

Figure 7 illustrates the magnetic field densities of the helical coils. Compared to the single-layer pipe coil, an increase in the number of turns along the z-axis results in a stronger magnetic field concentration around the wire winding. Additionally, it is observed that the decrease in magnetic field intensity toward the inner radius is less pronounced than toward the outer radius.

### B. Tubular Coil

Inductance can be defined as the rate of change of current that results from a wire's opposition to the current flowing through it. It varies depending on the characteristics and dimensions of the designed coil. The inductance values of the tubular coil, created using a single-layer helical coil design, are presented in Table 3.

The analysis was carried out by forming four different matrices expressing the variations in self-inductance and mutual inductance values based on the distance between two coils. Accordingly, the self-inductance value of the receiver coil was simulated at intervals of 50 millimeters, ranging from 50 mm to 200 mm. It was observed that the self-inductance of the receiver coil increased by a negligible amount (in microhenries) as the distance increased, leading to the conclusion that self-inductance is generally not a distance-dependent parameter.

When examining the inductance variables between the two coils, it was found that increasing the distance between the receiver and transmitter coils from 50 mm to 200 mm reduced their mutual interaction, resulting in a decrease in inductance values. While the mutual inductance was approximately 288 nanohenries at a 50 mm distance, it dropped to around 40 nanohenries as the distance increased.

The designed receiver and transmitter coils have identical properties, only simulated in different circuits. The four matrices generated include analyses of the receiver coil itself, the transmitter coil itself, the influence of the receiver on the transmitter coil, and vice versa. As shown in Table 3, the effect of the receiver coil on the transmitter coil is the same as that of the transmitter coil on the receiver. These mutual inductance values between the coils are referred to as mutual inductance.

Table 3. Inductance values of the tubular coil based on distance

Dist [mm]	Matrix1.L(Rx_in,Rx_in) [uH]	Matrix1.L(Tx_in,Rx_in) [nH]	Matrix1.L(Rx_in,Tx_in) [nH]	Matrix1.L(Tx_in,Tx_in) [uH]
50	1,059,284,195	2,883,624,008	2,883,624,008	1,027,905,872
100	1,077,048,379	1,347,104,723	1,347,104,723	1,027,939,357
150	1,084,632,573	7,238,513,311	7,238,513,311	1,027,926,006
200	1,090,609,133	407,477,378	407,477,378	1,027,982,918

The coupling coefficient is a value that expresses the interaction between the magnetic fields formed between two coils, and the symbol  $k$  represents it. This coefficient ranges between 0 and 1. Current flows through a coil and generates magnetic flux along the wire. The coupling coefficient has reached a sufficient level if the generated flux can connect with the other coil. In other words, when the coefficient is 1 (the ideal case), it indicates maximum interaction between the two coils, whereas when the coefficient is 0, it means there is no interaction between them at all. As seen in Table 4, which was created based on simulation

results, the coupling coefficient—and thus the magnetic field interaction between the coils—decreases as the distance between them increases.

Table 4. Coupling coefficient of the tubular coil based on distance

Dist [mm]	Matrix1.CplCoef (Rx_i,Rx_in)	Matrix1.CplCoef (Tx_in,Rx_in)	Matrix1.CplCoef (Rx_in,Tx_in)	Matrix1.CplCoef (Tx_in,Tx_in)
50	1	0,276347	0,276347	1
100	1	0,128026	0,128026	1
150	1	0,0685.531	0,0685.531	1
200	1	0,0384.836	0,0384.836	1

Figure 8 presents the graphical representation of Table 4. For the analysis of the graph, the X-axis represents the distance between 50 millimeters and 200 millimeters, while the Y-axis is scaled for coupling coefficient values ranging from 0 to 0.3. The most ideal point regarding distance and magnetic field efficiency is the midpoint of the graph. This optimal point occurs at a coupling coefficient between 0.09 and 0.1, corresponding to an approximate distance of 125 millimeters between the coils.

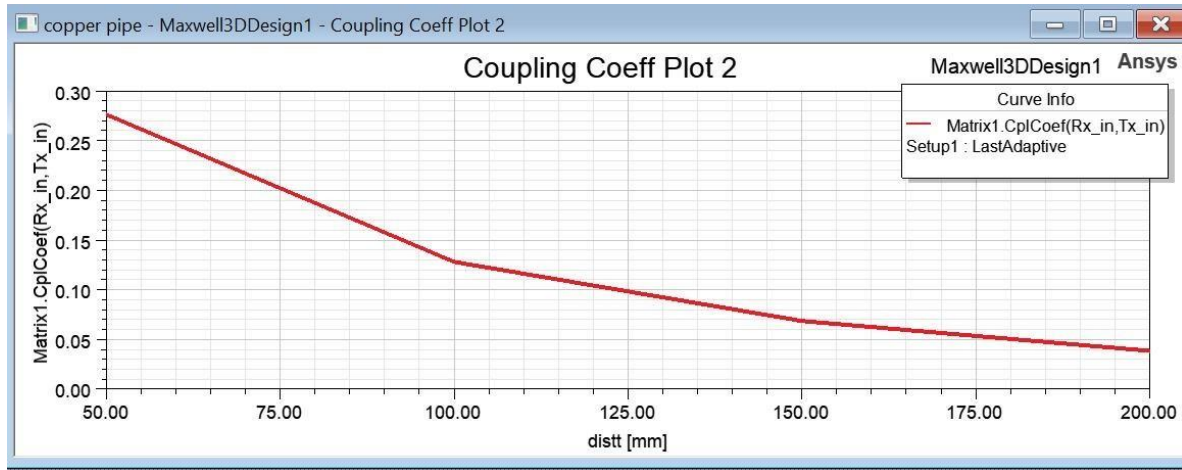


Fig 8. Graph of the coupling coefficient of the tubular coil based on distance

#### IV. CONCLUSION

The paper presents a comparative analysis of helical and tubular coils in terms of inductance and coupling coefficient across varying distances. Although self-inductance stays mostly invariant, the levels of mutual inductance and the coupling coefficient diminish with increasing distance. The helical coil exhibited modest coupling at 135 mm, whereas the tubular coil provided enhanced coupling at reduced distances. These results emphasize the significance of coil shape and placement in the design of effective inductive systems.

#### ACKNOWLEDGMENT

The authors express their science appreciation for the support received from the Smart Grids Laboratory at Istanbul Sabahattin Zaim University.

## REFERENCES

- [1] Rashid, M. H., *Power electronics handbook*. Butterworth-Heinemann, 4<sup>th</sup> Ed., 2017.
- [2] Chhawchharia, S., Sahoo, S. K., Balamurugan, M., Sukchai, S., & Yanine, F. "Investigation of wireless power transfer applications with a focus on renewable energy." *Renewable and Sustainable Energy Reviews*, 91, 888-902, 2018.
- [3] Krainyukov, A., Krivchenkov, A., & Saltanovs, R. "Performance analysis of wireless communications for V2G applications using WPT technology in energy transfer." *Procedia Engineering*, 178, 172-181, 2017.
- [4] Wadi, M., Elmasry, W., Jouda, M., Shahinzadeh, H., & Gharehpetian, G. B. "Overview of Electric Vehicles Charging Stations in Smart Grids." *13th International Conference on Computer and Knowledge Engineering (ICCKE)*, 2023, (pp. 540-546).
- [5] Peng, J., Zhang, L., Chen, Q., Long, R., Zhou, K., Liu, Z., & Su, H. "Anti-disturbance TUBE MPC method of wireless power transmission system based on state feedback." *Energy Reports*, 7, 411-418, 2021.
- [6] Wadi, M., Shobole, A., Elmasry, W., & Kucuk, I. "Load frequency control in smart grids: A review of recent developments." *Renewable and Sustainable Energy Reviews*, 189, 114013, 2024.
- [7] Wadi, M., Shobole, A., Tur, M. R., & Baysal, M. "Smart hybrid wind-solar street lighting system fuzzy based approach: Case study Istanbul-Turkey." *6th international Istanbul smart grids and cities congress and fair (ICSG)*, 2019, (pp. 71-75).
- [8] Wadi, M., & Elmasry, W. "An anomaly-based technique for fault detection in power system networks." *International Conference on Electric Power Engineering-Palestine (ICEPE-P)*, 2021, (pp. 1-6).
- [8] Elmasry, W., & Wadi, M. "EDLA-EFDS: A novel ensemble deep learning approach for electrical fault detection systems." *Electric Power Systems Research*, 207, 107834, 2022.
- [9] Wadi, M. "Fault detection in power grids based on improved supervised machine learning binary classification." *Journal of Electrical Engineering-Elektrotechnicky Casopis*, 2021.
- [10] Elmasry, W., & Wadi, M. "Detection of faults in electrical power grids using an enhanced anomaly-based method." *Arabian Journal for Science and Engineering*, 47(11), 14899-14914, 2022.
- [11] Elmasry, W., & Wadi, M. "Enhanced Anomaly-Based Fault Detection System in Electrical Power Grids." *International Transactions on Electrical Energy Systems*, 2022(1), 1870136, 2022.
- [12] Shobole, A., Wadi, M., Tür, M. R., & Baysal, M. "Real time active power control in smart grid." *IEEE 6th International Conference on Renewable Energy Research and Applications (ICRERA)*, 2017, (pp. 585-590).
- [13] Wadi, M. "Five different distributions and metaheuristics to model wind speed distribution." *Journal of Thermal Engineering*, 7(Supp 14), 1898-1920, 2021.
- [14] Wadi, M., & Elmasry, W. "Modeling of wind energy potential in Marama region using different statistical distributions and genetic algorithms." *International Conference on Electric Power Engineering-Palestine (ICEPE-P)*, 2021, (pp. 1-7).
- [15] Wadi, M., Kekezoglu, B., Baysal, M., Tur, M. R., & Shobole, A. "Feasibility study of wind energy potential in turkey: Case study of Catalca district in Istanbul." *2nd International Conference on Smart Grid and Renewable Energy*, 2019, (pp. 1-6).
- [16] Wadi, M., & Baysal, M. "Reliability assessment of radial networks via modified RBD analytical technique." *Sigma Journal of Engineering and Natural Sciences*, 35(4), 717-726, 2017.
- [17] Wadi, M., Elmasry, W., Shobole, A., Tur, M. R., Bayindir, R., & Shahinzadeh, H. "Wind energy potential approximation with various metaheuristic optimization techniques deployment." *7th International Conference on Signal Processing and Intelligent Systems (ICSPIIS)*, 2021, (pp. 1-6).
- [18] Elaydi, H., Jaddu, H., & Wadi, M. "An iterative technique for solving nonlinear optimal control problems using Legendre scaling function." *International Journal of Emerging Technology and Advanced Engineering*, 2(6), 7-11, 2012.
- [19] Tür, M. R., Wadi, M., Shobole, A. A., & Gündüz, H. "Integration problems of photovoltaic systems-wind power, solutions and effects on power quality." *European Journal of Technique (EJT)*, 10(2), 340-353, 2021.
- [20] Wadi, M., Baysal, M., & Shobole, A. "Reliability and sensitivity analysis for closed-ring distribution power systems." *Electric Power Components and Systems*, 49(6-7), 696-714, 2022.
- [21] Tur, M. R., Shobole, A., Wadi, M., & Bayindir, R. "Valuation of reliability assessment for power systems in terms of distribution system, A case study." *IEEE 6th International Conference on Renewable Energy Research and Applications (ICRERA)*, 2017, (pp. 1114-1118).
- [22] Wadi, M., Elmasry, W., & Tamyigit, F. A. "Important considerations while evaluating wind energy potential." *Journal of the Faculty of Engineering and Architecture of Gazi University*, 38(2), 947-962, 2023.
- [23] Elmasry, W., Wadi, M., & Shahinzadeh, H. "Two-tier cascaded classifiers to improve electrical power quality." *26th International Electrical Power Distribution Conference (EPDC)*, 2022, (pp. 96-101).
- [24] Wadi, M., Elmasry, W., Çolak, İ., Jouda, M., & Kucuk, I. "Utilizing metaheuristics to estimate wind energy integration in smart grids with a comparative analysis of ten distributions." *Electric power components and systems*, 1-36, 2024.
- [25] Wadi, M., Elmasry, W., Kucuk, I., & Shahinzadeh, H. "Sensitivity reliability analysis of power distribution networks using fuzzy logic." *12th International Conference on Computer and Knowledge Engineering (ICCKE)*, 2022, (pp. 190-195).
- [26] Wadi, M. "An empirical investigation into wind energy modeling: a case study utilizing five distributions and four advanced optimization methods." *Power Electronics Converters and their Control for Renewable Energy Applications* (pp. 237-263). Academic Press, 2023.
- [27] Wadi, M., Jouda, M., Salemedeb, M., & Husain, N. "PV Systems Efficiency Evaluation Using Machine Learning Techniques." *8th International Artificial Intelligence and Data Processing Symposium (IDAP)*, 2024, (pp. 1-7).



- [28] Salemdeeb, M., & Wadi, M. "Estimation of Solar Systems Energy Generation Based on Machine Learning." *8th International Artificial Intelligence and Data Processing Symposium (IDAP)*, 2024, (pp. 1-6).
- [29] Wadi, M., Salemdeeb, M., Jouda, M., Tur, M. R., Ayachi, B., & Husain, N. "PV Systems Generation Prediction Considering Cloud Cover Using Deep Learning Techniques." *Global Energy Conference (GEC)*, 2024, (pp. 215-221).
- [30] Jouda, M., & Wadi, M. "Design a Boost DC-DC Switching Luo Converter with a Single MOSFET Switch." *8th International Artificial Intelligence and Data Processing Symposium (IDAP)*, 2024, (pp. 1-6).
- [31] Wadi, M., & Elmasry, W. "Comparison of five different distributions based on three metaheuristics to model wind speed distribution." *Journal of Electrical Systems*, 2022.
- [32] Jouda, M., Wadi, M., Salemdeeb, M., & Tur, M. R. "Optimized Output Impedance for Parallel Inverters in Microgrids Utilizing ABC Algorithm and Droop Control Method." *Global Energy Conference (GEC)*, 2024, (pp. 353-358).
- [33] Jouda, M., & Wadi, M. "IoT with LoRa Architecture for Indoor Air Quality Monitoring System." *8th International Artificial Intelligence and Data Processing Symposium (IDAP)*, 2024, (pp. 1-6).
- [34] Wadi, M., Tamiğit, F. A., Husain, N., & Küçük, İ. AI Applications in Electrical and Electronics Engineering. *Innovations of Artificial Intelligence in Electrical and Electronics Engineering*, 2025.
- [35] Ali, A., Wadi, M., & Jouda, M. Cybersecurity in Smart Grids and Other Application Fields. *Innovations of Artificial Intelligence in Electrical and Electronics Engineering*, 2025.
- [36] Alabsi, A., Hawbani, A., Wang, X., Al-Dubai, A., Hu, J., Aziz, S. A., ... & Alsamhi, S. H. "Wireless power transfer technologies, applications, and future trends: A review." *IEEE Transactions on Sustainable Computing*, 2024.
- [37] Zavrel, M., Kindl, V., Frivaldsky, M., & Skala, B. "Dynamic wireless power transfer in E-mobility using AC power bus and matrix converter: implementation suitability study." *Electrical Engineering*, 1-9, 2025.
- [38] Lee, B., Kim, J., Jo, H., Min, H., & Bien, F. "Arrangement Free Wireless Power Transfer via Strongly Coupled Electrical Resonances." *Advanced Science*, 12(2), 2407827, 2025.
- [39] Onreabroy, W., Piemsomboon, S., Traikunwaranon, S., Wilaiprajuabsang, N., & Kaewpradap, A. "Enhancing Wireless Power Transfer Efficiency Through Innovative Metamaterial Configurations for Electric Vehicles." *World Electric Vehicle Journal*, 16(1), 48, 2025.
- [40] Yilmaz, U. "Improved a two-stage control method for efficient wireless power transfer in fuel cell applications." *Renewable Energy*, 240, 122219, 2025.
- [41] Shobole, A. A., & Wadi, M. "Multiagent systems application for the smart grid protection." *Renewable and Sustainable Energy Reviews*, 149, 111352, 2021.
- [42] Tur, M. R., Wadi, M., Shobole, A., & Ay, S. "Load frequency control of two area interconnected power system using fuzzy logic control and PID controller." *7th International Conference on Renewable Energy Research and Applications (ICRERA)*, 2018, (pp. 1253-1258).
- [43] Wadi, M., Baysal, M., & Shobole, A. "Comparison between open-ring and closed-ring grids reliability." *4th International Conference on Electrical and Electronic Engineering (ICEEE)*, 2017, (pp. 290-294).
- [44] Wadi, M., Baysal, M., Shobole, A., & Tur, M. R. "Reliability evaluation in smart grids via modified Monte Carlo simulation method." *7th International Conference on Renewable Energy Research and Applications (ICRERA)*, 2018, (pp. 841-845).
- [45] Costantino, T., Miretti, F., & Spessa, E. "Assessing the viability of dynamic wireless power transfer in long-haul freight transport: A techno-economic analysis from fleet operators' standpoint." *Applied Energy*, 379, 124839, 2025.
- [46] Ouaridhine A., Aissat A., Wadi M., Grouni S., Benammar MA. "The Impact of Emitter Thickness on the Performance of Silicon PIN Single-Junction Solar Cells", *4th International Conference on Contemporary Academic Research*, 2025, 459-462.
- [47] Ouaridhine A., Aissat A., Wadi M., Grouni S., Benammar MA. "The Effect of Varying Absorber Width in a PIN Polysilicon Solar Cell Structure on The Absorption Coefficient", *4th International Conference on Contemporary Academic Research*, 2025, 463-466.